The Spatial Evolution of Clusters in Massive MIMO Mobile Measurement at 3.5 GHz

Chao Wang*, Jianhua Zhang*, Lei Tian*, Mengmeng Liu*, and Ye Wu†
*Key Laboratory of Universal Wireless Communications, Ministry of Education, Wireless Technology Innovation Institute,
Beijing University of Posts and Telecommunications, P.O. box # 92, China, 100876
†Huawei Technologies Co., Ltd.
Email: {chaowang, jhzhang}@bupt.edu.cn

***Abstract*—It is necessary to study the spatial evolution of clusters in massive multiple-input multiple-output (MIMO) mobile channel, which is one of the important features in cluster-based models. In this paper, we analyze the data collected from the massive MIMO mobile measurement campaign, with a 256-element virtual array at 3.5 GHz in line of sight (LoS) and non line of sight (NLoS) conditions, respectively. Firstly, the cluster-level angular power spectrums (APS), azimuth of departure (AoD) and azimuth of arrival (AoA), are shown to display the variation of clusters along with the measurement route. Secondly, the evolution of cluster number is presented, showing the changes of appearance and disappearance of the clusters, and the corresponding model based on birth-death process is built. Finally, the cumulative density functions (CDF) of radii of visibility regions (VR) are calculated, which are used to study the variations of VRs along with the measurement route, and lognormal distribution fits the CDFs well.**

I. Introduction

Channel modelling plays an indispensable role in the research of wireless communications. In 4G era, many measurement campaigns have been conducted for conventional multiple-input multiple-output (MIMO), following by theoretical analysis to study the cluster characteristics and cluster-level modelling in mobile scenarios [**?** **?** **?** **?**]. Cluster is defined as a group of multipath components (MPCs) with similar parameters, e.g., angle of arrival (AoA), angle of departure (AoD), and delay. It simplifies the number of channel parameters and constitutes the basis of geometry-based stochastic channel models (GBSM). In [**?**], the average number of clusters in indoor office environments is proposed, which shows the active cluster number in different positions. [**?**] reports the lifetimes of clusters in indoor-to-outdoor and outdoor-to-indoor environments, which is directly related to the size of visibility region (VR), while [**?**] reports them in an indoor hall environment. [**?**] proposes an evolution model of cluster number from dynamic double-directional measurements in indoor environment, and uses cluster-level parameters to describe the dynamic channel.

Compared to the current state of the art, massive MIMO has a large number of antennas, typically in the order of hundreds, which can provide better performance in efficiency, capacity, reliability and etc [**?** **?** **?**]. Considering this, more and more work is turning to the massive MIMO technology. So a series of massive MIMO measurement campaigns have been performed to evaluate the channel performance, e.g., in [**?**], outdoor channel measurements at 2.6 GHz with a linear virtual array and a cylindrical array of 128-element antenna are reported, which study the sum-rate capacity, spectrum efficiency, precoding schemes and etc. In [**?**], an outdoor static measurement performed in a stadium with a linear 128-element antenna virtual array at 1.4725 GHz, and the angular power spectrum (APS) in massive MIMO channel is analyzed.

With the increasing number of antennas, the clusters would probably change in angle domain and quantity. However, to the best knowledge of authors, there is still no relevant study on evolution of clusters in the massive MIMO mobile channel measurement. Another relevant cluster-level parameters, like VR, would change, too. VR is an assumed circular region given in the area. When the mobile station (MS) moves inside one VR, the corresponding clusters would be active. Otherwise, it would be inactive. So it is an important parameter to observe the existence of active clusters during the movement.

Considering this, a new massive MIMO mobile measurement campaign in urban macro (UMa) scenario, including line of sight (LoS) and non line of sight (NLoS) propagation conditions, with a 256-element virtual antenna array at 3.5 GHz and 200 MHz bandwidth are designed and performed. In this paper, the spatial evolution of clusters and the corresponding VRs are analyzed. The properties of clusters can present the time-variant and spatially-variant nature of MIMO channels. And the concept of VR is suitable to model the time-variant and spatial-variant channels due to the movement of MS. We can get a direct insight of the spatial evolution of clusters during movement by observing these parameters.

The rest of the paper is organized as follows. In Section II, the channel measurement setup, the method of data extraction and processing are described in detail. In Section III, the data analysis are presented. APSs in LoS and NLoS conditions are shown. And the evolution of cluster number is presented, then we make a model to simulate it based on birth-death process. Also the radii of visibility regions are calculated. Finally, the conclusions are drawn in Section IV.

II. Measurement Setup and Data Processing

To observe the evolution of clusters in the mobile measurement campaign of massive MIMO, we performed virtual measurement to form the large antenna array. Then the collected data was used to do further observation and analysis. All the

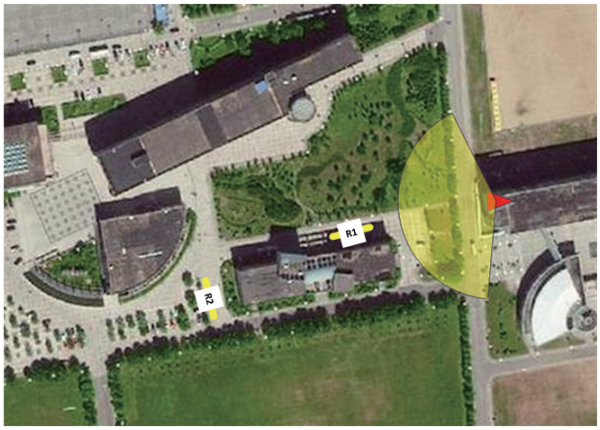

Fig. 1. The overview of the measurement area by Baidu Map (The red point is the Tx side, two yellow lines, R1 and R2, represent the measurement route in LoS and NLoS conditions, respectively)

details of the experiment setup, the method of data extraction and processing are shown in the following.

A. Measurement Description

The channel measurement campaign was performed in the Hongfu Campus, Beijing University of Posts and Telecommunications, China (see Fig. 1). We used the Elektrobit Propsound channel sounder with a carrier frequency of 3.5 GHz and 200 MHz bandwidth, to collect the raw data of channel impulse response (CIR). In the Tx side, a 32-element uniform planar array (UPA) was used, shown in Fig. 2 (a). At the MS side, the dual-polarized omnidirectional array (ODA) has 56-element antenna and in this case, #1 - #16 antennas were chosen for measurement campaign (see Fig. 2 (b)). The specific parameters of the measurement are listed in Table I.

To form the massive MIMO array with 256 antennas, a virtual measurement method was adopted. Fig. 3 shows the scheme of 256-element combining antenna array, giving 8 positions. And we combined 8 collecting data groups into one, formed the 256-element antenna array equivalent data. The rationality of the virtual measurement was proved in [**?**], the power delay profile (PDP) calculated from combined CIRs and CIRs collected from the measurement campaigns can fit well. Also the spatial angular characteristics, the elevation angle of departure (EoD), azimuth of departure (AoD), elevation angle of arrival (EoA) and azimuth of arrival (AoA), which are estimated from the combination match well with those from measurement campaigns.

In the measurement, we pushed the MS along with the 8 m rail (see Fig. 4 (a)) with a constant speed of about 1.4 m/s to simulate the mobility of user terminals. The Tx side was put on the roof of the building in the east (see Fig. 4 (b)). And the measurement campaign was performed in UMa scenario, two routes were designed, corresponding to the LoS and NLoS scenarios, respectively. The route, R1, moving from the east to the west, has LoS conditions. And R2, moving from the north to the south, has NLoS conditions obviously, which is mainly blocked by the teaching building.

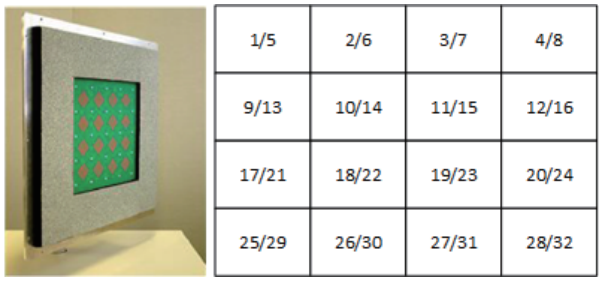

(a) Tx: 4×4 patches with each patch comprising a pair of cross-polarized antennas.

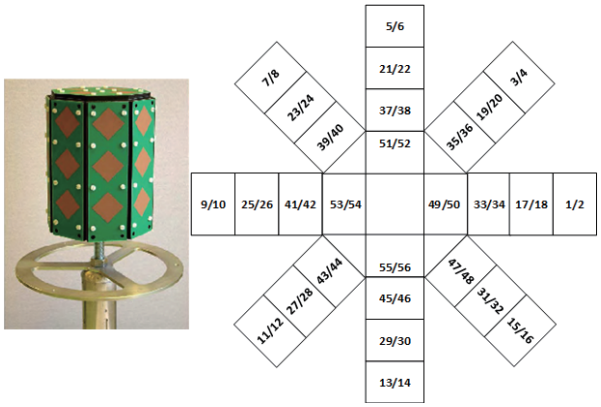

(b) Rx: 8 adjacent sides with 3 patches each, a top surface with 4 patches, each patch contains a pair of cross-polarized antennas.

Fig. 2. Antenna layouts used in the measurement

TABLE I
THE SPECIFICATIONS OF MEASUREMENT CAMPAIGN

Parameter		Value	
Antenna type		ODA (Rx)	UPA (Tx)
Number of antenna ports		56(16 ports were used)	32
Overall radiation pattern		Omnidirectional	Hemispherical
Inter element spacing		41.0 mm	41.0 mm
Number of elements		28	16
Polarized		$\pm 45^{\circ}$	$\pm 45^{\circ}$
Angle range	Azimuth	$-180^{o} \sim 180^{o}$	$-70^{o} \sim 70^{o}$
	Elevation	$-70^{o} \sim 90^{o}$	$-70^{o} \sim 70^{o}$
Center frequency		3.5 GHz	
Bandwidth		200 MHz	
PN sequence		255 chips	

B. Data Processing

Firstly, we need to do some preprocessing, reordering the 8 groups of CIRs sequences to one group of sequences. Secondly, the space-alternating generalized expectation maximization (SAGE) algorithm was used to estimate the channel parameters from the raw data [**?**], which provides a joint estimation of parameter set $\theta_l = \{\tau_l, f_{d,l}, \Phi_l, \Omega_l, \alpha_l\}$, $l = \{1, \ldots, L\}$. The τ_l, $f_{d,l}$, Φ_l, Ω_l and α_l denote the propagation delay, the

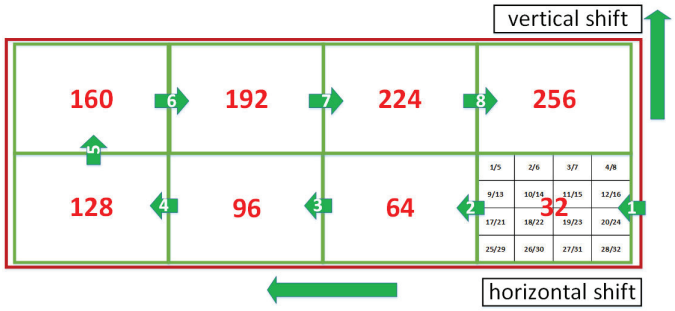

Fig. 3. The scheme of the antenna combining array in the virtual measurement

(a) MS (b) Tx

Fig. 4. MS and Tx

doppler shift, the angle of departure, the angle of arrival and polarization of the lth propagation subpath, respectively. Specifically, $\Phi_l = [\theta_{T,l}, \phi_{T,l}]$, $\Omega_l = [\theta_{R,l}, \phi_{R,l}]$, where $\theta_{T,l}$, $\phi_{T,l}$, $\theta_{R,l}$ and $\phi_{R,l}$ denote the EoD, AoD, EoA and AoA, respectively. Finally, we group them to the level of clusters for further study, which is also the basis of all recent GBSM, from COST 259 to WINNER II. In our analysis, the Kpower-Means clustering algorithm was used to group the multipath components (MPC) with similar properties into a series of clusters [**?**].

III. Data Analysis

A. Angular Power Distribution

The angular power distribution shows the movement of MS and the evolution of clusters. After processing the raw data, the channel properties can be shown in cluster level. Fig. 5 and Fig. 6 show the two of cluster-level APSs of AoD and AoA in LoS and NLoS conditions, respectively. In these figures, every point represents the spatial position of one cluster, X-coordinate represents distance from the starting point of the rail, Y-coordinate represents the angular degree of the cluster, and the color of the points represents the normalized power of clusters.

A clear strong path can be seen in Fig. 5 (a) and Fig. 5 (b), the clusters' AoD focus on around $0°$ while AoA focus on around $-25°$. This main path is formed by the LoS conditions, most of clusters focus on it. Although there are some MPCs in other degrees in both figures, their normalized power is low, shown in the color of dark blue.

In Fig. 6 (a), rich clusters distribute ranging from $-80°$ to $80°$. In Fig. 6 (a), most of clusters focus on around $38°$ while

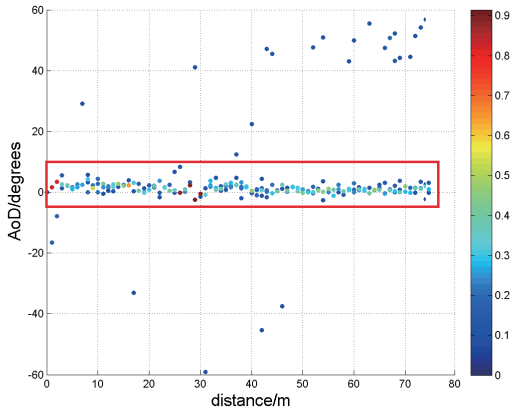

(a) AoD

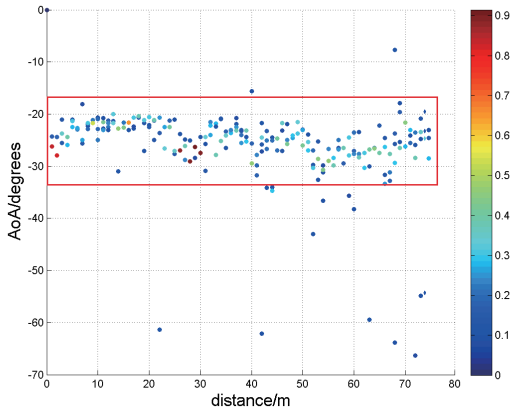

(b) AoA

Fig. 5. The cluster-level APSs in LoS conditions, most of clusters focus on the main path.

clusters mainly focus on around $-48°$ in Fig. 6 (b). This is because most of transmitting waves reflected by the fan-shaped building on the left of the route. When the MS moves to the distance ranging from 2.5 m to 5 m, the number of clusters become more (see in Fig. 6 (a)). A similar phenomenon can be seen in the case of AoA, when the MS moves to the distance ranging from 2.5 m to 5 m, clusters become more, also this phenomenon can be observed in Fig. 7. This is because R2 was perpendicular to the transmitting waves. During the movement, MS experienced changing scattering environments. At the distance ranging from about 2.5 m to 5 m, MS was closed to some shrubs. Because of this, clusters' power and angles vary all the time during the movement. And some clusters appear or disappear in some positions along with the route, e.g., one cluster appears at (3.8, 80.69), and disappears at (6.3, 78) in Fig. 6 (b).

It is noted that it is hard to keep the speed of the MS completely same in every measurement campaign. Thus, every time the length of the collecting data sequences has slightly differences. To ensure the SAGE results are correct, these 8 groups of time sequences should be kept at one alignment. The redundant part of sequences were cut down among these

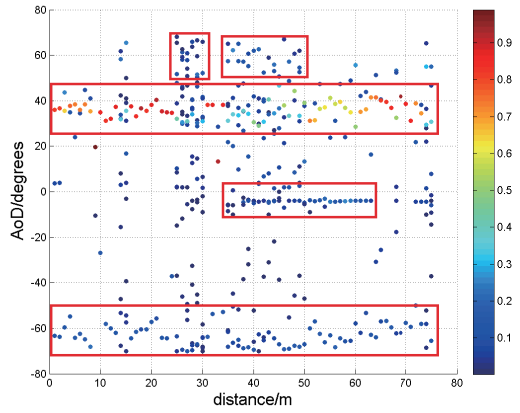

(a) AoD

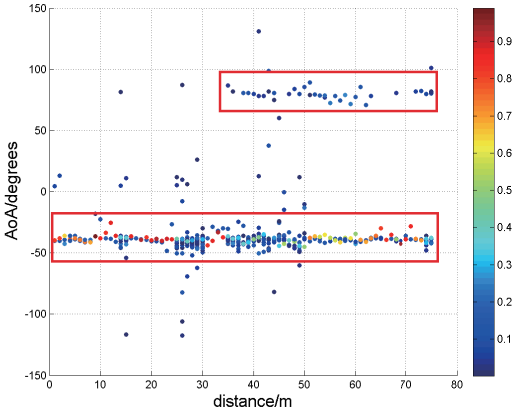

(b) AoA

Fig. 6. The cluster-level APSs in NLoS conditions, clusters distribute in different degrees.

groups to form the one group. This is why there is no data point when the value of the X-axis >7.6 m.

B. The Evolution of Cluster Number

The evolution of clusters present the spatial variation of the massive MIMO channel during the movement. When the MS moves, the power of different clusters varies, some clusters appear or disappear. Based on the result of clustering, we can get the cluster number evolution (see in Fig. 7) in R1 (LoS) and R2 (NLoS). The blue curve represents the LoS conditions, with average number of clusters is 13.7867, and when the distance is 0.5 m, it gets the largest cluster number, 20. While in NLoS conditions (red curve in Fig. 7), the average number is 5.8533, and the largest number is 17 with the distance of 2.9 m and 3 m, so the cluster number in LoS conditions is more than that in NLoS conditions. This is because the cluster power is normalized, some MPCs' normalized power is too low to keep for clustering. In addition, the cluster number changes more sharply in NLoS conditions than in LoS conditions.

Considering the features of clusters, the evolution of cluster number based on birth-death process is simulated, which can reflect the non-stationary properties of the clusters. The

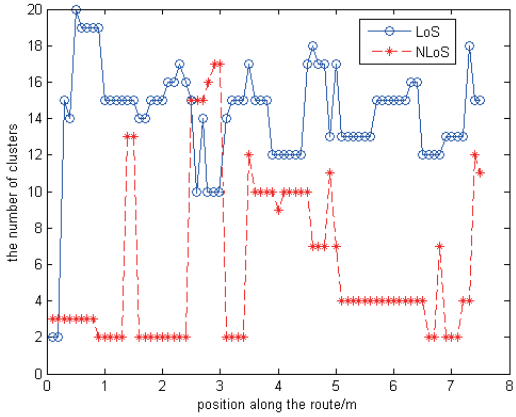

Fig. 7. The evolution of clusters along with the measurement route (blue curve represents the LoS conditions, while red curve represents the NLoS conditions)

evolution of clusters is expressed as

$$C(i) \xrightarrow{E} C(i+1)\,(i = 1, 2, \cdots, R) \tag{1}$$

where *R* is the evolution number, it depends on the length of measurement route L and observation spacing δ_R along with the route, e.g., the length of route is 8 m, and the observation spacing is set as 0.1 m, so evolution number *R* is 80.

According to [**?**], the process of birth and death is assumed to be statistic independent, since the time variation of the channel can also be reflected when MS moves. And the main variable in this model is the distance. The birth and death probability of each cluster are respectively expressed as

$$\lambda_i = \lambda e^{-\lambda \delta_R D} \tag{2}$$

$$\mu_i = \mu e^{-\mu \delta_R D} \tag{3}$$

where λ is the cluster newly-generate rate, μ is the cluster disappear rate, δ_R is the observation spacing, and D is the distance correlation factor. And the birth-death process should meet the following conditions

$$\begin{cases} p_{ii+1}(t) = \lambda_i(t) + o(t), (\lambda_i > 0, i = 0, 1, ..., N-1, \lambda_N = 0) \\ p_{ii-1}(t) = \mu_i(t) + o(t), (\mu_i > 0, i = 1, 2, ..., N, \mu_0 = 0) \\ p_{ii}(t) = 1 - (\lambda_i + \mu_i)t + o(t) \\ p_{ij}(t) = o(t), |i - j| \geqslant 2 \end{cases} \tag{4}$$

Thus, we use these to evolve the cluster set $C(i)$, which is consist of $\{c_1, c_2, \cdots, c_R\}$. Based on this, the evolution of cluster number can be stimulated. Fig. 8 (a) shows an example of evolution of cluster number by simulation, different clusters appear or disappear in different positions, such as the 17th cluster, which appears at 5.3 m and disappears at 7.3 m. Fig. 8 (b) gives the simulated evolution of cluster number, the number changes more sharply in the NLoS conditions than those in LoS conditions, and the average number is lower in NLoS

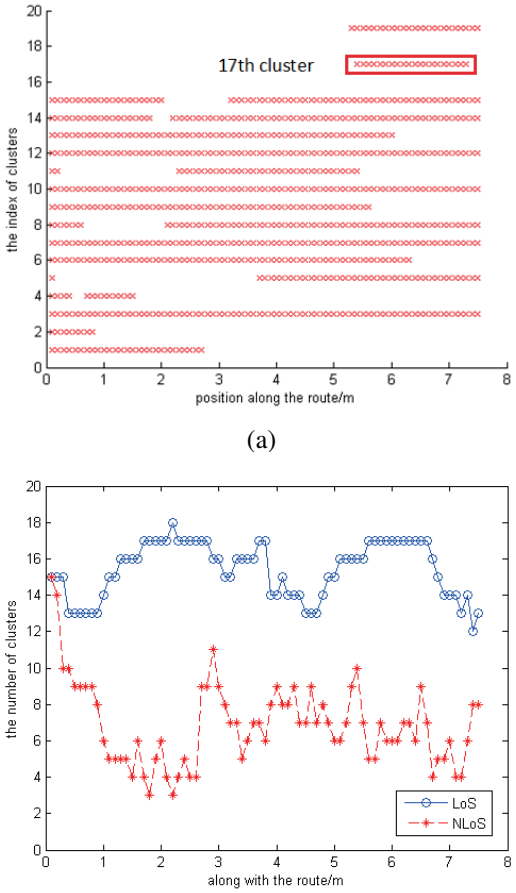

Fig. 8. An example of clusters' evolution based on birth-death process. (λ = 0.98, μ = 0.01, δ_R = 0.1 m, D = 1.3). (a) cluster evolution along with the measurement route by simulation (b) the evolution of cluster number in LoS and NLoS by simulation (blue curve represents the LoS conditions, while red curve represents the NLoS conditions)

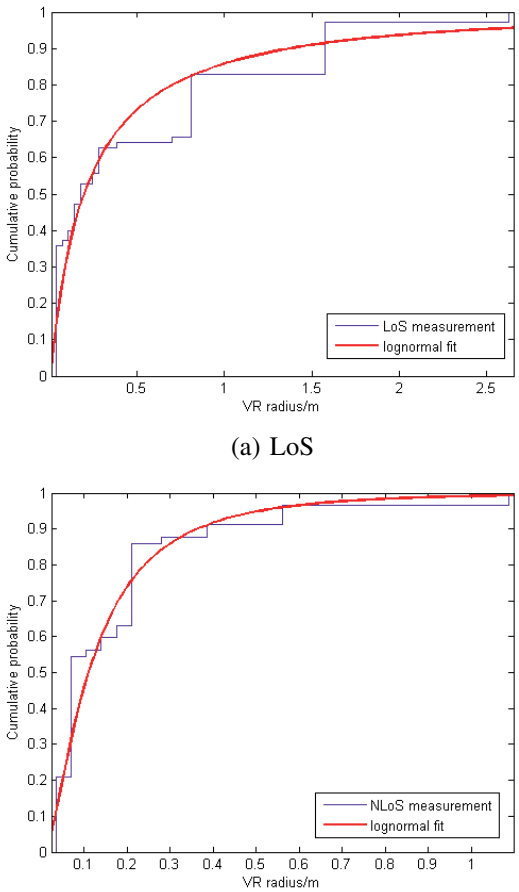

Fig. 9. The CDFs of radii of VRs in LoS and NLoS conditions, respectively (purple curves represent the measurement analysis, while the red curves represent the fitted curves by lognormal distribution).

conditions than that in LoS conditions, which are similar with the measurement results.

C. Visibility Regions

The concept of VR is proposed by the COST 259, COST 2100 MIMO channel model and so on [**? ?**]. It is an assumed circular region given in the area, each VR is related to only one cluster. When the MS moves inside one VR, the corresponding clusters would be active. Otherwise, it would be inactive. With these features, clusters can be observed clearly in mobile scenarios.

Based on the results of clustering, we inferred and calculated the lifetimes of clusters by converting lifetime to the radius of VR [**?**], and the cumulative density functions (CDF) of radii of the VRs are presented. To simplify the method, we assume that the MS moves across the center of VRs, i.e., all of the circle centers are distributed along with the route. As shown in Fig. 9 (a), in LoS conditions, the radii of VRs range from 0.03 m to 2.63 m. And in Fig. 9 (b), the radii in NLoS conditions range from 0.03 m to 1.0871 m, which are less than those in LoS conditions, because the appearance and disappearance of clusters would occur more frequently. And the lognormal distribution fitting is built, with respect to the measurement curves. the mean and standard deviation of the fitting curve is calculated, 0.5180 m and 0.6505 m in LoS conditions and 0.1778 m and 0.2187 m in NLoS conditions, respectively (see in Fig. 9). The parameters of data analysis are listed in the Table II.

IV. Conclusion

In this paper, a series of cluster-based analyses for massive MIMO mobile measurement campaign, based on the 256-element virtual array at 3.5 GHz, in LoS and NLoS conditions, are presented, respectively. Firstly, the cluster-level APSs, are plotted, clusters mainly appear or disappear in one path in LoS conditions, while those distribute in different degrees in NLoS conditions. The variation of clusters present the changing scattering environment clearly. Then we plot the evolution of cluster number along with the route, the number of clusters in NLoS conditions is less than that in LoS conditions, and the cluster number changes more sharply. In the meantime, we model the evolution by birth-death process,

TABLE II
THE PARAMETERS OF DATA ANALYSIS

Parameter		LoS	NLoS
the radius of VR	μ	0.5180	0.1778
	σ	0.4231	0.0478
	Max	2.63	1.0871
the fitted lognormal distribution	μ	-1.6324	-2.1994
	σ	1.5242	0.9261

the simulation result fit the measurement well. Finally, the CDFs of radii of VRs and the fitted curves by lognormal distribution are presented. With these shown parameters, we can get a direct insight of the spatial evolution of clusters during the movement. It provides a point of reference for wireless channel conditions in mobile scenario.

ACKNOWLEDGMENT

This research is supported in part by National Science and Technology Major Project of the Ministry of Science and Technology (2014ZX03003013), and in part by National Key Technology Research and Development Program (2012BAF14B01), and in part by National Natural Science Foundation of China (61322110, 6141101115), and by 863 Program (2015AA01A703) and Doctoral Fund of Ministry of Education (201300051100013). This research is also supported by Huawei Technologies Co., Ltd.

REFERENCES

[1] N. Czink, X. Yin, H. Özcelik, M. Herdin, E. Bonek, and B. H. Fleury, "Cluster characteristics in a MIMO indoor propagation environment," *IEEE Trans. on Wireless Commun.*, Vol. 6, No. 4, April 2007, pp. 1465-1475.

[2] L. Hentilä, M. Alatossava, N. Czink, and P. Kyösti, "Cluster-level parameters at 5.25 GHz indoor-to-outdoor and outdoor-to-indoor MIMO radio channels", *in Proc. 16th IST Mobile and Wireless Commu. Summit*, July 2007, pp. 1-5.

[3] J. Poutanen, K. Haneda, J. Salmi, V. M. Kolmonen, F. Tufvesson and P. Vainikainen, "Analysis of radio wave scattering processes for indoor MIMO channel models," *2009 IEEE 20th International Symp. on Personal, Indoor and Mobile Radio Commu.*, Tokyo, 2009, pp. 102-106.

[4] J. Poutanen, K. Haneda, J. Salmi, V. M. Kolmonen and P. Vainikainen, "Modeling the evolution of number of clusters in indoor environments," *Proc. of the 4th Euro. Conf. on Antennas and Prop.*, Barcelona, Spain, 2010, pp. 1-5.

[5] X. Gao, O. Edfors, F. Rusek, and F. Tufvesson, "Massive MIMO performance evaluation based on measured propagation data," *IEEE Trans. Wireless Commun.*, vol. 14, no. 7, pp. 3899-3911, Jul. 2015

[6] J. Zhang, C. Pan, F. Pei, G. Liu and X. Cheng, "Three-dimensional fading channel models: A survey of elevation angle research," *IEEE Commun. Mag.*, vol. 52, no. 6, pp. 218-226, June 2014.

[7] E. G. Larsson, O. Edfors, F. Tufvesson, and T. L. Marzetta, "Massive MIMO for next generation wireless systems," *IEEE Commun. Mag.*, vol. 52, no. 2, pp. 186-195, Feb. 2014.

[8] X. Gao, F. Tufvesson and O. Edfors, "Massive MIMO channels - Measurements and models," *2013 Asilomar Conf. on Sig., Systems and Comp.*, Pacific Grove, CA, 2013, pp. 280-284.

[9] W. Li, L. Liu, C. Tao, Y. Lu, J. Xiao and P. Liu, "Channel measurements and angle estimation for massive MIMO systems in a stadium," *2015 17th International Conf. on Advanced Commu. Tech. (ICACT)*, Seoul, 2015, pp. 105-108.

[10] H. Yu, J. Zhang, Q. Zheng, Z. Zheng, L. Tian and Y. Wu, "The rationality analysis of masssive MIMO virtual measurement at 3.5 GHz", *2016 Workshop, IEEE International Conf. on Comp. and Commu.* (ICCC Workshop), in press.

[11] B. Fleury, M. Tschudin, R. Heddergott, D. Dahlhaus, and K. Ingeman Pedersen, "Channel parameter estimation in mobile radio environments using the SAGE algorithm," *IEEE J. Sel. Areas in Commun.*, vol. 17, no. 3, pp. 434-450, Mar. 1999.

[12] N. Czink, *The Random-Cluster Model - A Stochastic MIMO Channel Model for Broadband Wireless Communication Systems of the 3rd Generation and Beyond.* Dissertation, Telecommunications Research Center Vienna (FTW), 2007.

[13] T. Zwick, C. Fischer, D. Didascalou, and W. Wiesbeck, "A stochastic spatial channel model based on wave-propagation modeling," *IEEE J. Sel. Areas Commun.*, vol. 18, no. 1, pp. 6-15, Jan. 2000.

[14] A. F. Molisch, H. Asplund, R. Heddergott, M. Steinbauer and T. Zwick, "The COST259 Directional Channel Model-Part I: Overview and Methodology," *IEEE Trans. on Wireless Commu.*, vol. 5, no. 12, pp. 3421-3433, Dec 2006.

[15] R. Verdone and A. Zanella, *Pervasive Mobile and Ambient Wireless Communications: COST Action 2100.* London, U.K.: Springer-Verlag, 2012.